Dephasing, decoherence, . . .

What is it all about ?

Decoherence of a single spin

Consider a spinor
(total phase is irrelevant)

$$\Psi = \begin{pmatrix} \psi_{\uparrow} e^{i\varphi} \\ \psi_{\downarrow} e^{-i\varphi} \end{pmatrix}$$

Average components of the spin can be expressed through the absolute values of the spinor's components and the phase

$$S_z = |\psi_{\uparrow}|^2 - |\psi_{\downarrow}| \qquad S_x = \sqrt{1 - S_z^2}\cos\varphi \qquad S_y = \sqrt{1 - S_z^2}\sin\varphi$$

Let us start with $S_z = 0, \quad \varphi = 0$, i.e. $\vec{S} \,||\, \vec{x}$ and apply magnetic field $\vec{B} \,||\, \vec{z}$ for some time interval Δt. Spin rotation $\Rightarrow \varphi \propto B\Delta t$

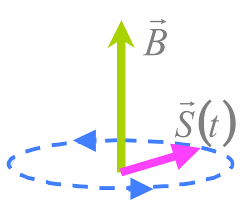

Coherent Oscillations of, e.g., x-projection of the spin (!?)

$$S_z = |\psi_\uparrow|^2 - |\psi_\downarrow| \qquad S_x = \sqrt{1 - S_z^2}\cos\varphi \qquad S_y = \sqrt{1 - S_z^2}\sin\varphi$$

Let us start with $S_z = 0, \quad \varphi = 0$, i.e. $\vec{S} \parallel \vec{x}$ and apply magnetic field $\vec{B} \parallel \vec{z}$ for some time interval Δt. Spin rotation ⇒ $\varphi \propto B\Delta t$

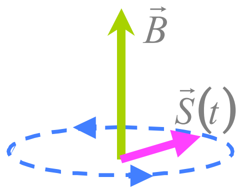

Coherent Oscillations of, e.g., x-projection of the spin (!?)

One can also apply time-independent field $\vec{B} \parallel \vec{x}$, that will cause the Zeeman splitting, and also a small oscillating in time field in $\vec{z}$ - direction, with the frequency close to the Zeeman splitting. There will be again rotation in xy -plane ⇒ Rabi oscillations

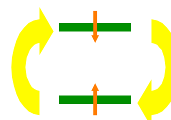

Decoherence of a single spin

Consider a spinor
(total phase is irrelevant)

$$\psi = \begin{pmatrix} \psi_\uparrow e^{i\varphi} \\ \psi_\downarrow e^{-i\varphi} \end{pmatrix}$$

Average components of the spin can be expressed through the absolute values of the spinor's components and the phase

$$S_z = |\psi_\uparrow|^2 - |\psi_\downarrow| \qquad S_x = \sqrt{1 - S_z^2}\cos\varphi \qquad S_y = \sqrt{1 - S_z^2}\sin\varphi$$

A random time-dependent magnetic field $\vec{B}(t)$ changes the phase in an uncontrollable way ⟷ it rotates the spin.

This can be called decoherence

Relaxation times T_1, T_2

letters to nature

NATURE IVOL 398 I 29 APRIL 1999

Coherent control of macroscopic q in a single-Co

Y. Nakamura*, Yu. A. Pashk

* NEC Fundamental Research Labor
† CREST, Japan Science and Technol
Saitama 332-0012, Japan

A nanometre-scale superconducting electrode connected to a reservoir via a Josephson junction constitutes an artificial two-level electronic system: a single-Cooper-pair box. The two levels consist of charge states (differing by $2e$, where e is the electronic charge) that are coupled by tunnelling of Cooper pairs through the junction. Although the two-level system is macroscopic, containing a large number of electrons, the two charge states can be coherently superposed[1–4]. The Cooper-pair box has therefore been suggested[5–7] as a candidate for a quantum bit or 'qubit'—the basic component of a quantum computer. Here we report the observation of quantum oscillations in a single-Cooper-pair box. By applying a short voltage pulse via a gate electrode, we can control the coherent quantum state evolution: the pulse modifies the energies of the two charge states non-adiabatically, bringing them into resonance. The resulting state—a superposition of the two charge states—is detected by a tunnelling current through a probe junction. Our results demonstrate electrical coherent control of a qubit in a solid-state electronic device.

Y. Nakamura*, Yu. A. Pashkin† & J. S. Tsai*

NATURE IVOL 398 I 29 APRIL 1999

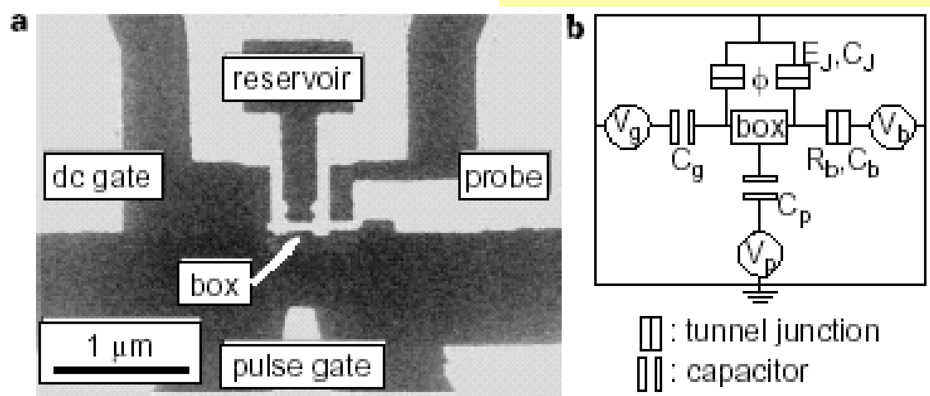

Figure 1 Single-Cooper-pair box with a probe junction. **a**, Micrograph of the sample. The electrodes were fabricated by electron-beam lithography and shadow evaporation of Al on a SiN_x insulating layer (400-nm thick) above a gold ground plane (100-nm thick) on the oxidized Si substrate. The 'box' electrode is a $700 \times 50 \times 15$ nm Al strip containing $\sim 10^8$ conduction electrons. The reservoir electrode was evaporated after a slight oxidation of the surface of the box so that the overlapping area becomes two parallel low-resistive tunnel junctions ($\sim$10 kΩ in total) with Josephson energy E_J which can be tuned through magnetic flux ϕ penetrating through the loop. Before the evaporation of the probe electrode we further oxidized the box to create a highly resistive probe junction ($R_b \approx 30$ MΩ). Two gate electrodes (d.c. and pulse) are capacitively coupled to the box electrode. The sample was placed in a shielded copper case at the base temperature ($T \approx 30$ mK; $k_B T \approx 3$ μeV) of a dilution refrigerator. The single-electron charging energy of the box electrode $E_C = e^2/2C_\Sigma$ was 117 ± 3 μeV, where C_Σ is the total capacitance of the box electrode. The superconducting gap energy Δ was 230 ± 10 μeV. **b**, Circuit diagram of the device. The Cs represent the capacitance of each element and the Vs are the voltage applied to each electrode.

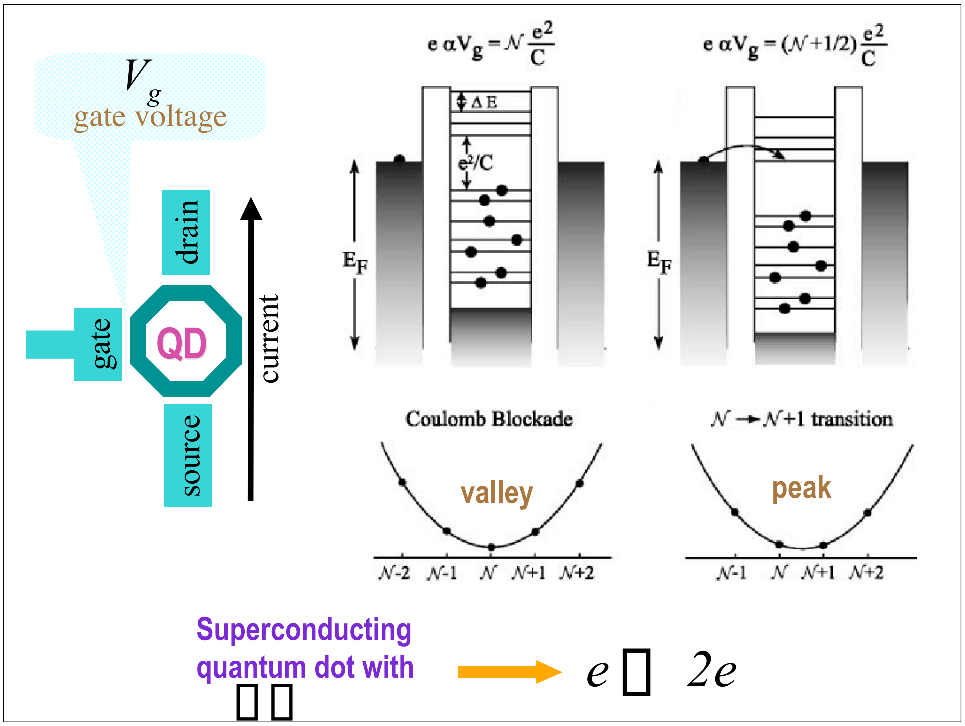

V_g
gate voltage
drain
gate
QD
source
current
$e\,\alpha V_g = \mathcal{N}\frac{e^2}{C}$
$e\,\alpha V_g = (\mathcal{N}+1/2)\frac{e^2}{C}$
ΔE
e^2/C
E_F
E_F
Coulomb Blockade
$\mathcal{N} \rightarrow \mathcal{N}+1$ transition
valley
peak
$\mathcal{N}$-2 $\mathcal{N}$-1 $\mathcal{N}$ $\mathcal{N}$+1 $\mathcal{N}$+2
$\mathcal{N}$-1 $\mathcal{N}$ $\mathcal{N}$+1 $\mathcal{N}$+2
Superconducting
quantum dot with
e 2e

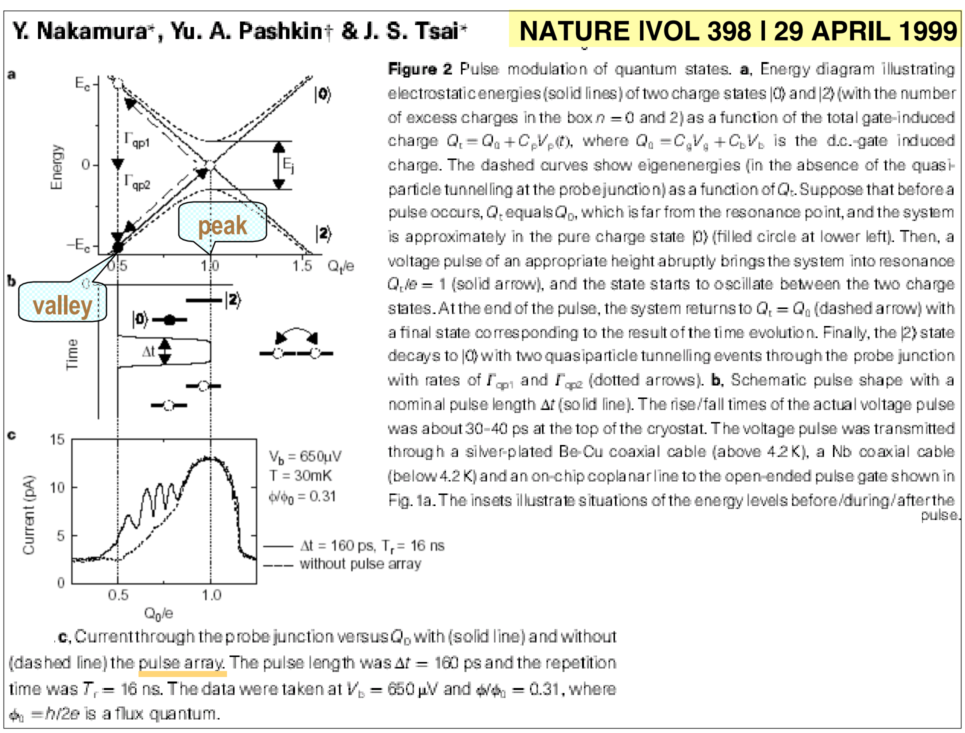

Y. Nakamura*, Yu. A. Pashkin† & J. S. Tsai*
NATURE I VOL 398 I 29 APRIL 1999
a
E_c
0
$-E_c$
Energy
Γ_{qp1}
Γ_{qp2}
E_J
|0⟩
|2⟩
peak
valley
0.5 1.0 1.5 Q_t/e
b
Time
|0⟩
|2⟩
Δt
c
Current (pA)
15 10 5 0
0.5 1.0
Q_0/e
V_b = 650μV
T = 30mK
ϕ/ϕ_0 = 0.31
Δt = 160 ps, T_r = 16 ns
without pulse array
Figure 2 Pulse modulation of quantum states. **a**, Energy diagram illustrating electrostatic energies (solid lines) of two charge states |0⟩ and |2⟩ (with the number of excess charges in the box $n = 0$ and 2) as a function of the total gate-induced charge $Q_t = Q_0 + C_pV_p(t)$, where $Q_0 = C_gV_g + C_bV_b$ is the d.c.-gate induced charge. The dashed curves show eigenenergies (in the absence of the quasi-particle tunnelling at the probe junction) as a function of Q_t. Suppose that before a pulse occurs, Q_t equals Q_0, which is far from the resonance point, and the system is approximately in the pure charge state |0⟩ (filled circle at lower left). Then, a voltage pulse of an appropriate height abruptly brings the system into resonance $Q_t/e = 1$ (solid arrow), and the state starts to oscillate between the two charge states. At the end of the pulse, the system returns to $Q_t = Q_0$ (dashed arrow) with a final state corresponding to the result of the time evolution. Finally, the |2⟩ state decays to |0⟩ with two quasiparticle tunnelling events through the probe junction with rates of Γ_{qp1} and Γ_{qp2} (dotted arrows). **b**, Schematic pulse shape with a nominal pulse length Δt (solid line). The rise/fall times of the actual voltage pulse was about 30–40 ps at the top of the cryostat. The voltage pulse was transmitted through a silver-plated Be-Cu coaxial cable (above 4.2 K), a Nb coaxial cable (below 4.2 K) and an on-chip coplanar line to the open-ended pulse gate shown in Fig. 1a. The insets illustrate situations of the energy levels before/during/after the pulse.
c, Current through the probe junction versus Q_0 with (solid line) and without (dashed line) the pulse array. The pulse length was Δt = 160 ps and the repetition time was T_r = 16 ns. The data were taken at V_b = 650 μV and ϕ/ϕ_0 = 0.31, where $\phi_0 = h/2e$ is a flux quantum.

Y. Nakamura*, Yu. A. Pashkin† & J. S. Tsai*

NATURE IVOL 398 I 29 APRIL 1999

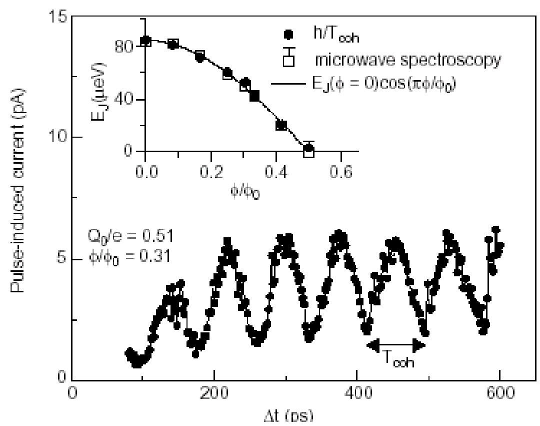

Figure 4 Pulse-induced current as a function of the pulse length Δt. The data correspond to the cross-section of Fig. 3a at $Q_0/e = 0.51$. Inset, Josephson energy E_J versus the magnetic flux ϕ penetrating through the loop. E_J was estimated by two independent methods. One was from the period of the coherent oscillation T_{coh} as h/T_{coh}. The other was from the gap energy observed in microwave spectroscopy[4]. The solid line shows a fitting curve with $E_J(\phi = 0) = 84\,\mu$eV assuming cosine ϕ-dependence of E_J.

Quantum oscillations in two coupled charge qubits

Yu. A. Pashkin, T. Yamamoto, O. Astafiev, Y. Nakamura, D. V. Averin & J. S. Tsai

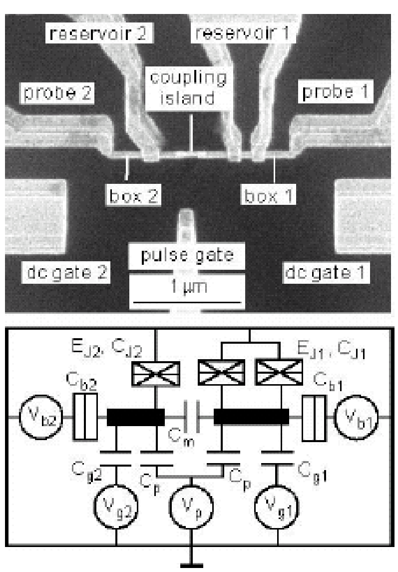

Figure 1. Two capacitively coupled charge qubits. **a**, Scanning electron micrograph of the sample. The qubits were fabricated by electron-beam lithography and three-angle evaporation of Al (light areas) on a SiN_x insulating layer (dark) (see ref.5 for fabrication details). Two qubits are coupled by an additional coupling island overlapping both Cooper-pair boxes. Although the coupling island has a finite tunnelling resistance ~ 10 MΩ to the boxes, we consider the coupling as purely capacitive represented by a single capacitor in the equivalent circuit because all the tunnelling processes are completely blocked. The estimated capacitance of the island to the ground is ~ 1 aF. **b**, Equivalent circuit of the device. The parameters obtained from the dc measurements are: $C_{J1} = 620$ aF, $C_{J2} = 460$ aF, $C_{b1} = 41$ aF, $C_{b2} = 50$ aF, $C_{g1} = 0.60$ aF, $C_{g2} = 0.61$ aF, $C_p \approx 1$ aF, $C_m = 34$ aF, and the corresponding energies are $E_{c1} = 484\,\mu$eV (117 GHz in frequency units), $E_{c2} = 628\,\mu$eV (152 GHz) and $E_m = 65\,\mu$eV (15.7 GHz). Josephson coupling energies, $E_{J1} = 55\,\mu$eV (13.4 GHz) and $E_{J2} = 38\,\mu$eV (9.1 GHz), were determined from the single qubit measurements described later in the text. Probe junction tunnel resistance is equal to 31.6 MΩ (left) and 34.5 MΩ (right). Superconducting energy gap is 210 μeV. Black bars denote Cooper-pair boxes. Symbol ⊟ represents a tunnel junction without Josephson coupling, while ⊠ is a Josephson tunnel junction.

Quantum oscillations in two coupled charge qubits

Yu. A. Pashkin, T. Yamamoto, O. Astafiev, Y. Nakamura, D. V. Averin & J. S. Tsai

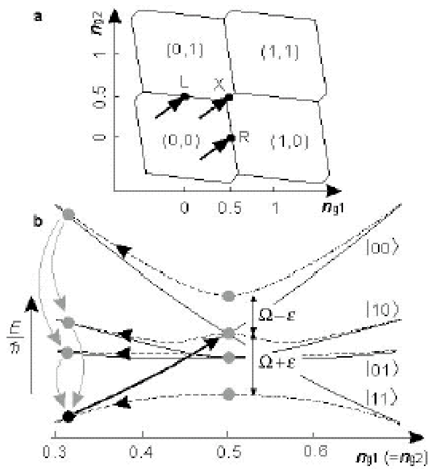

Figure 2. Pulse operation of the device. **a**, Schematics of the ground-state charging diagram of the coupled qubits as a function of the normalised gate charges n_{g1} and n_{g2}. The number of Cooper pairs n_1 and n_2 in the neighbouring cells differs by one. The electrostatic energies E_{n1n2} are degenerate at the boundaries. Points R and L correspond to energy degeneracy in the first and the second qubit, respectively. Point X is doubly degenerate: $E_{00} = E_{11}$ and $E_{10} = E_{01}$. Arrows show how pulses shift the system in the experiment. **b**, Energy diagram of the system along the line $n_{g1} = n_{g2}$ through the point X. Solid lines are the electrostatic energies of charge states |00>, |10>, |01> and |11>. Dashed lines are eigenenergies of the Hamiltonian (1). Far from co-resonance (point X in **a**), the system stays in |00>. After the pulse brings the system to the co-resonance (solid arrow), the system starts to evolve producing a superposed state $|\psi(t)\rangle = c_1|00\rangle + c_2|10\rangle + c_3|01\rangle + c_4|11\rangle$. The amplitudes $|c_i|$ (i = 1, 2, 3, 4) remain "frozen" after the pulse termination (dashed arrows) until the resulting state decays into the ground state. The decay process indicated by grey arrows contributes to the probe currents proportional to the probabilities (3).

Quantum oscillations in two coupled charge qubits

Yu. A. Pashkin, T. Yamamoto, O. Astafiev, Y. Nakamura, D. V. Averin & J. S. Tsai

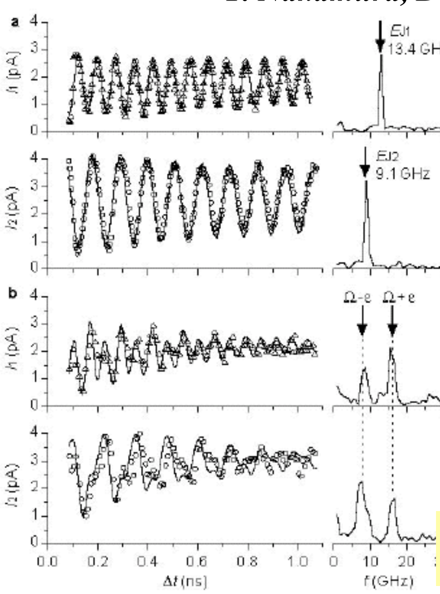

Figure 3. Quantum oscillations in qubits. **a**, Probe current oscillations in the first (top) and the second (bottom) qubit when the system is driven to the points R and L, respectively. Right panel shows corresponding spectra obtained by the Fourier transform. In both cases, the experimental data (open triangles and open dots) can be fitted to a cosine dependence (solid lines) with an exponential decay with 2.5 ns time constant. **b**, Probe current oscillations in the qubits at the co-resonance point X. Their spectra (right panel) contain two components. Arrows and dotted lines indicate the position of Ω + ε, Ω - ε obtained from (3) using E_{J1}=13.4 GHz, E_{J2}=9.1 GHz measured in the single qubit experiments (Fig. 3a) and E_m=15.7 GHz estimated independently from dc measurements. Solid lines are fits obtained from numerical simulation with the parameters E_{J1}=13.4 GHz, E_{J2}=9.1 GHz and E_m=14.5 GHz. Finite pulse rise/fall time and not pure |00> initial condition were taken into account. The introduced exponential decay time is 0.6 ns.

decoherence times $\tau_{coupled} \approx \frac{1}{4}\tau_{uncoupled}$

What is Dephasing?

1. Suppose that originally a system(an electron) was in a *pure* quantum state. It means that it could be described by a **wave function** with a given phase.

2. External perturbations can transfer the system to a different quantum state. Such a transition is characterized by its amplitude, which has a modulus and a phase.

3. The phase of the amplitude can be measured by comparing it with the phase of another amplitude of the same transition.

Example: Fabri-Perrot interferometer

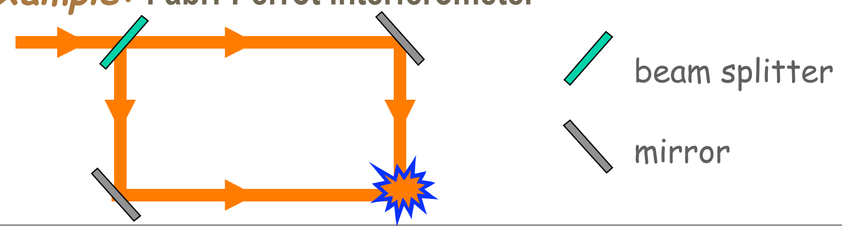

4. Usually we can not control all of the perturbations. As a result, even for fixed initial and final states, the phase of the transition amplitude has a random component.

5. We call this contribution to the phase, $\delta\varphi$, random if it changes from measurement to measurement in an uncontrollable way.

6. It usually also depends on the duration of the experiment, t:

$$\delta\varphi = \delta\varphi(t)$$

7. When the time t is large enough, $\delta\varphi$ exceeds 2π, and interference gets averaged out.

8. Definitions:

$$\delta\varphi(\tau_\varphi) \approx 2\pi$$

τ_φ phase coherence time; $1/\tau_\varphi$ dephasing rate

Why is Dephasing rate important?

Imagine that we need to measure the energy of a quantum system, which interacts with an environment and can exchange energy with it.

Let the typical energy transferred between our system an the environment in time t be $\delta\varepsilon(t)$. The total uncertainty of an ideal measurement is

$$\delta E(t) \approx \delta\varepsilon(t) + \frac{\hbar}{t}$$

environment

quantum uncertainty

$\delta\varepsilon(t)$ [illegible] ;
$\frac{\hbar}{t}$ [illegible] $t \to 0$ [illegible]

There should be an optimal measurement time $t=t^*$, which minimizes $\delta E(t)$:
$\delta E(t^*) = \delta E_{min}$

! $\delta\varepsilon(t^*) \approx \frac{\hbar}{t^*}$ ⇒ $\delta\varepsilon(t^*) \approx 1$ ⇒ $t^* \approx \tau_\varphi$, $\delta E_{min} \approx \hbar/\tau_\varphi$!

Why is Dephasing rate important?

$\delta\varepsilon(t^*) \approx \frac{\hbar}{t^*}$ ⇒ $\delta\varepsilon(t^*) \approx 1$ ⇒ $t^* \approx \tau_\varphi$, $\delta E_{min} \approx \hbar/\tau_\varphi$

It is dephasing rate that determines the accuracy at which the energy of the quantum state can be measured in principle

How to detect phase coherence / measure the dephasing/decoherence rate ?

Quantum phenomena in electronic systems:

- Weak localization
- Mesoscopic fluctuations
- Persistent current
- Orthogonality catastrophe

} later

-
-

Magnetoresistance

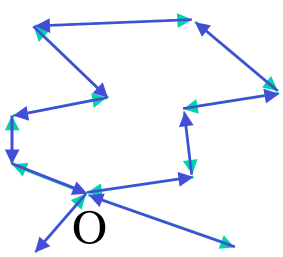

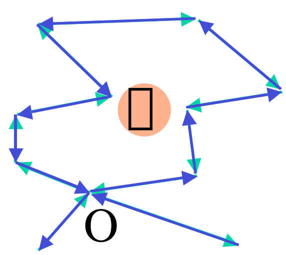

No magnetic field $\varphi_1 = \varphi_2$

With magnetic field H $\varphi_1 - \varphi_2 = 2\pi \, 2\Phi/\Phi_0$

$\Phi = HS$ - *magnetic flux through the loop* $\Phi_0 = hc/e$ - *flux quantum*

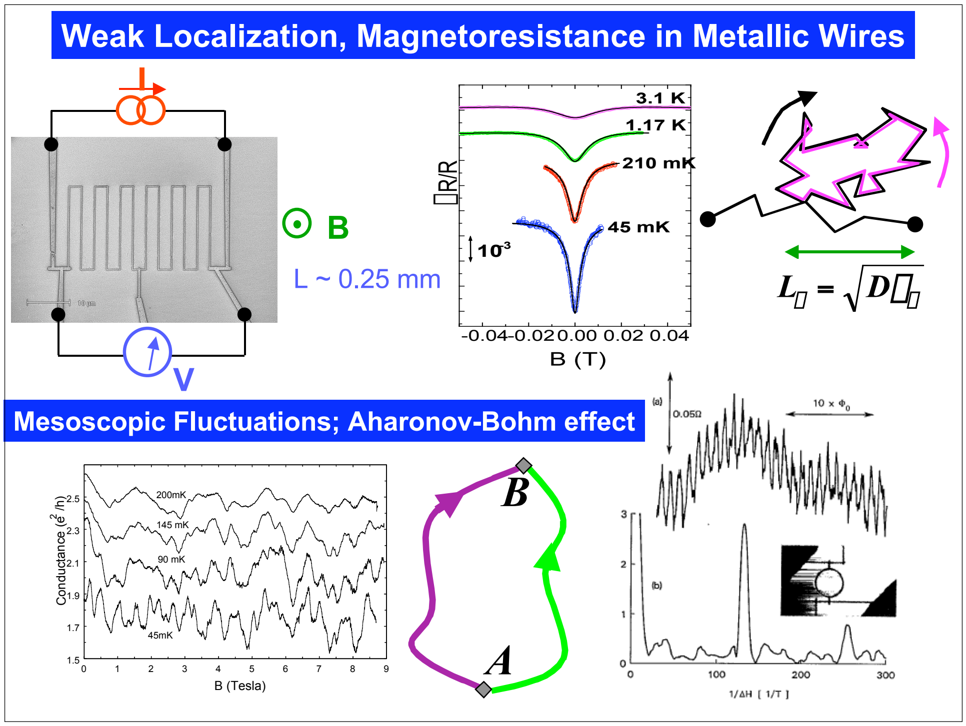

Can we reliably extract the dephasing rate from the experiment

Is energy transfer necessary for the "dephasing" **?**

Weak localization:

NO - *everything that violates T-invariance will destroy the constructive interference*

EXAMPLE: *random quenched magnetic field*

Mesoscopic fluctuations:

YES - *Even strong magnetic field will not eliminate these fluctuations. It will only reduce their amplitude by factor* **2.**

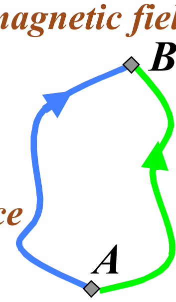

Therefore

Statistical analysis is unavoidable if we want to experimentally determine the dephasing rate

On the other hand

Let the random potential change in time very slowly, but still quick on the scale of measurement time

Weak localization:

Averaging over different realizations of the disorder

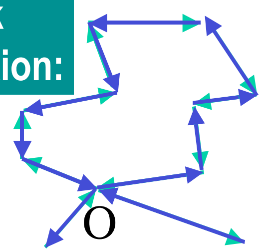

At any moment

$\square_1 = \square_2$

Mesoscopic fluctuations:

Averaging over time

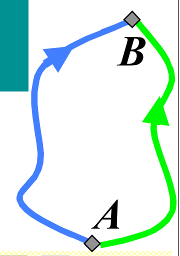

$\square_1 \square \square_2$

Is time dependent

Therefore

Weak localization effects do not feel the motion of impurities

Mesoscopic fluctuations get suppressed

Magnetic Impurities

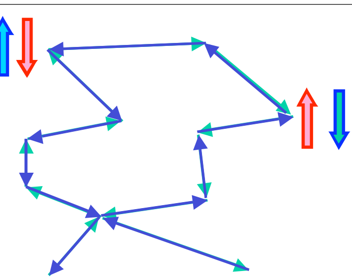

⇑ - before ⇑ - after

T-invariance is clearly violated, therefore we have dephasing

Mesoscopic fluctuations

Magnetic impurities cause dephasing only through effective interaction between the electrons.

T□ 0 *Either Kondo scattering or quenching due to the RKKY exchange.*

In both cases no "elastic dephasing"

Long time (spin) dynamics in metallic (spin) glasses ?

VOLUME 88, NUMBER 4 PHYSICAL REVIEW LETTERS 28 JANUARY 2002

Charge Echo in a Cooper-Pair Box

Y. Nakamura,[1] Yu. A. Pashkin,[2,*] T. Yamamoto,[1] and J. S. Tsai[1]
[1]*NEC Fundamental Research Laboratories, Tsukuba, Ibaraki 305-8501, Japan*
[2]*CREST, Japan Science and Technology Corporation (JST), Kawaguchi, Saitama, 332-0012 Japan*
(Received 5 September 2001; published 8 January 2002)

A spin-echo-type technique is applied to an artificial two-level system that utilizes a charge degree of freedom in a small superconducting electrode. Gate-voltage pulses are used to produce the necessary pulse sequence in order to eliminate the inhomogeneity effect in the time-ensemble measurement and to obtain refocused echo signals. Comparison of the decay time of the observed echo signal with an estimated decoherence time suggests that low-frequency energy-level fluctuations due to the 1/*f* charge noise dominate the dephasing in the system.

Charge Echo in a Cooper-Pair Box

Y. Nakamura,[1] Yu. A. Pashkin,[2] T. Yamamoto,[1] and J. S. Tsai[1]

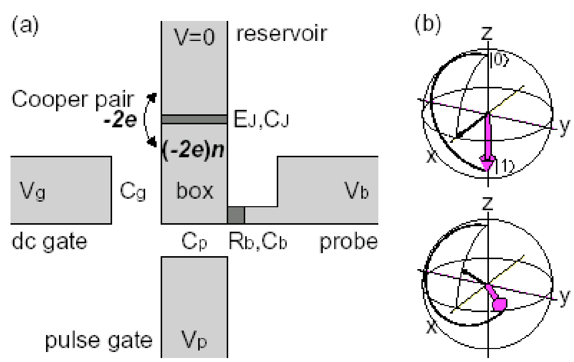

FIG. 1. (a) Schematic of a Cooper-pair box with an additional probe electrode. (b) Bloch sphere representations of schematic quantum-state evolutions at $Q_0 = 0.45e$ corresponding to the two pulse heights $\Delta Q_p = 0.55e$ (top) and $\Delta Q_p = 0.53e$ (bottom). The thin arrow in the xz-plane indicates the direction of the effective magnetic field.

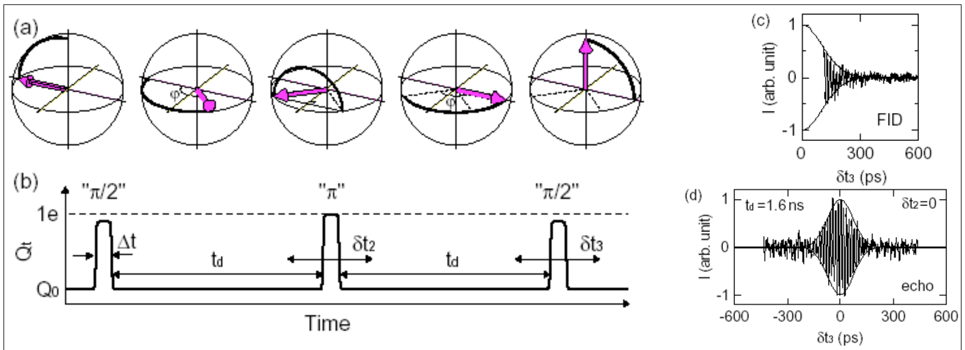

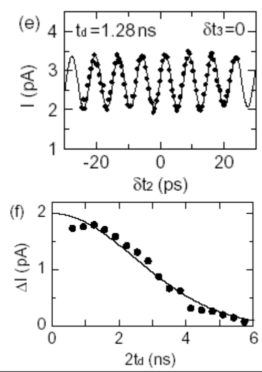

FIG. 2. Charge-echo experiment: (a) Schematic quantum-state evolutions. (b) Pulse sequence. (c) Normalized free-induction decay (FID) signal vs. δt_3 taken without the second pulse and with $t_d = 0$. The oscillating signal is highpass-filtered and normalized to the gaussian envelope $\exp(-(\delta t_3/150\text{ps})^2)$. (d) Normalized echo signal vs. δt_3. The envelope is $\exp(-(\delta t_3/100\text{ps})^2)$. The signal-to-noise ratio is poor, because the data was taken with three "($\frac{\pi}{2}$)"-pulses instead of the ideal pulse sequence. T_r is 64 ns in (c) and (d). (e) Echo-signal current I vs. δt_2. Solid curve is a sinusoidal fit. (f) Oscillation amplitude of the echo-signal current ΔI as a function of $2t_d$ with a gaussian fit.

Decoherence factor

$$\frac{I_{\max}(\tau)}{I_{\max}(0)} \equiv e^{-D(\tau)}$$

Let the spacing between the two levels, ΔE, fluctuate in time:

$$\delta E(t) \equiv \Delta E - \langle \Delta E \rangle$$

random phase

$$\varphi(\tau) = \frac{1}{\hbar}\int_0^{\tau} \delta E(t)\,dt \quad \Rightarrow \quad e^{-D(\tau)} = \left\langle e^{i\varphi(\tau)} \right\rangle$$

Assume that $\delta E(t)$ is gaussian, and

$$\langle \delta E(0)\,\delta E(t) \rangle_{\omega} \equiv S_{\delta E}(\omega)$$

$$D(\tau) = \frac{1}{2\hbar^2}\int_{\omega_m} S_{\delta E}(\omega)\left[\frac{\sin(\omega\tau/2)}{\omega/2}\right]^2 d\omega$$

ω_m is inverse time of the measurement

Decoherence factor

$$\frac{I_{\max}(\tau)}{I_{\max}(0)} \equiv e^{-D(\tau)}$$

For the free induction decay

$$D_{FID}(\tau) = \frac{1}{2\hbar^2}\int_{\omega_m} S_{\delta E}(\omega)\left[\frac{\sin(\omega\tau/2)}{\omega/2}\right]^2 d\omega$$

For the echo signal

$$D_{echo}(\tau) = \frac{1}{2\hbar^2}\int_{\omega_m} S_{\delta E}(\omega)\left[\frac{\sin^2(\omega\tau/4)}{\omega/4}\right]^2 d\omega$$

At $\omega \to 0$

$$\left[\frac{\sin(\omega\tau/2)}{\omega/2}\right]^2 \to const \qquad \left[\frac{\sin^2(\omega\tau/4)}{\omega/4}\right]^2 \propto \omega^2$$

Even $\omega << \tau^{-1}$ are important

Low frequency fluctuations are not important

Decoherence factor

$$\frac{I_{\max}(\tau)}{I_{\max}(0)} \equiv e^{-D(\tau)}$$

$$D_{FID}(\tau) = \frac{1}{2\hbar^2}\int_{\omega_m} S_{\delta E}(\omega)\left[\frac{\sin(\omega\tau/2)}{\omega/2}\right]^2 d\omega$$

$$D_{echo}(\tau) = \frac{1}{2\hbar^2}\int_{\omega_m} S_{\delta E}(\omega)\left[\frac{\sin^2(\omega\tau/4)}{\omega/4}\right]^2 d\omega$$

$$\langle \delta E(0)\delta E(t)\rangle_\omega \equiv S_{\delta E}(\omega)$$

1/f noise: $S_{\delta E}(\omega) \propto \frac{1}{\omega}$

$$D_{FID}(\tau) \propto \tau^2 \log\left(\frac{1}{\omega_m \tau}\right)$$

$$D_{echo}(\tau) \propto \tau^2$$

$\approx \log(10^9) >> 1$

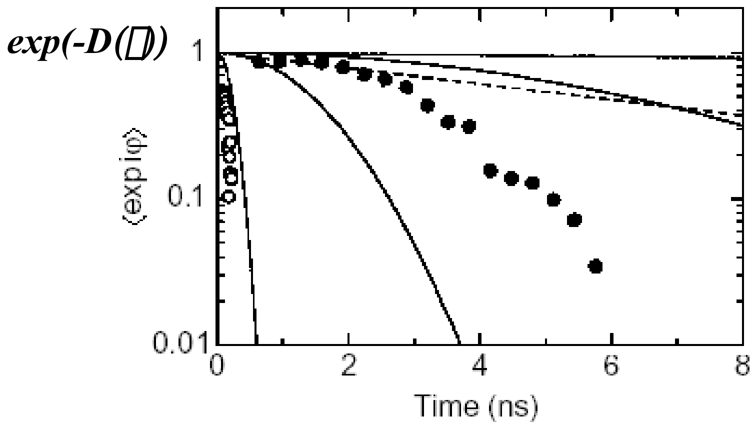

FIG. 3. Decay of the normalized amplitude of the echo signal (filled circles) and the FID signal (open circles) compared with estimated decoherence factors $\langle \exp i\varphi \rangle$ due to electromagnetic environment (dotted line), the read-out process (dashed), and $1/f$ charge noise with $\alpha = (1.3 \times 10^{-3} e)^2$ (dash-dotted). Two solid lines are estimations for the echo experiment in the presence of the same $1/f$ charge-noise spectrum (bottom) and that with $\alpha = (3.0 \times 10^{-4} e)^2$ (top).

Q: $\omega \ll \tau^{-1}$ How can so slow change of the energy splitting cause any decoherence, if ΔE is practically a constant during the process of quantum oscillations. **?**

A: It is not a true decoherence.

It is rather a **temporally inhomogeneous** broadening:

Different shots cause oscillations with slightly **different frequencies**

The echo technique allows one to get rid of the **temporally inhomogeneous** broadening:

$$D_{echo}(\tau) \propto \int_{\omega_m} \left[\frac{\sin^2(\omega\tau/4)}{\omega\tau/4} \right]^2 \frac{d\omega}{\omega}$$

This integral is determined by ω of the order of τ^{-1}

Decoherence factor

$$\frac{I_{\max}(\tau)}{I_{\max}(0)} \equiv e^{-D(\tau)}$$

Let the spacing between the two levels, ΔE, fluctuate in time:

$$\delta(t) \equiv \Delta E - \langle \Delta E \rangle$$

Gate error

What is the origin of the 1/*f* noise?

1. One fluctuator (e.g., 2 level system) - telegraph noise. Time-dependent dipole moment $d(t)$:

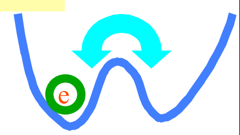

$$\langle d(0)d(t)\rangle \propto \exp(-\gamma t) \xrightarrow{\text{Fourier transform}} \frac{\gamma}{\omega^2+\gamma^2}$$

2. Several fluctuators with different values of the relaxation rate γ:

$$\langle \delta(0)\delta(t)\rangle_\omega \propto \sum_i C_i \frac{\gamma_i}{\omega_i^2+\gamma_i^2} \xrightarrow{\text{Ensemble averaging}} \langle C\rangle \int P(\gamma)\frac{\gamma}{\omega^2+\gamma^2}\,d\gamma$$

C_i is the coupling constant of the i-th fluctuator, and $<C>$ is its mean value. $P(\gamma)$ is the probability density of the relaxation rates. We assumed that C_i and γ are statistically independent

3. Assuming now that $\log(\gamma)$ is distributed uniformly (it is natural if $\gamma \propto \exp(-S)$), i.e., $P(\gamma) \propto 1/\gamma$ we obtain

$$\langle \delta(0)\delta(t)\rangle_\omega \propto \frac{1}{\omega}$$

B.A. & B. Z. Spivak, **JETP Letters, v. 49, #8, p. 527 (1989)**
"Fluctuations in the intensity of 1/*f* noise in disordered metals"

$$\langle \square(0)\square(t)\rangle_{\square} \quad \square_i C_i \frac{\square_i}{\square_i^2 + \square_i^2}$$

C_i is the coupling constant
$\square_i$ is the relaxation rate
$\square(\square) \equiv \square E \; \square \langle \square E \rangle$

For a small system (qubit) each contribution, $\square_i(\square)$, is inverse proportional to the cube of the distance, r, between the system and the fluctuating dipole moment: $\square_i(\square) \quad d(\square)/r^3$

The decoherence is dominated by a single fluctuator.

Telegraph noise

$$D(\square) \quad \begin{cases} \square^3 & \square\square < 1 \\ \square & \square\square > 1 \end{cases}$$

1/f noise

$$D(\square) \quad \square^2$$

Different fluctuators dominate at different □

The decoherence is dominated by a single fluctuator.

$$D(\square) \quad \begin{cases} \square^3 & \square\square < 1 \\ \square & \square\square > 1 \end{cases}$$

Telegraph noise

$$D(\square) \quad \square^2$$

1/f noise

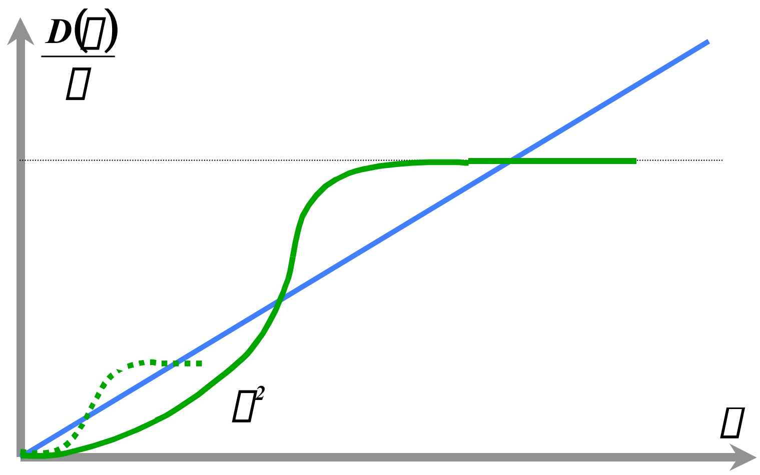

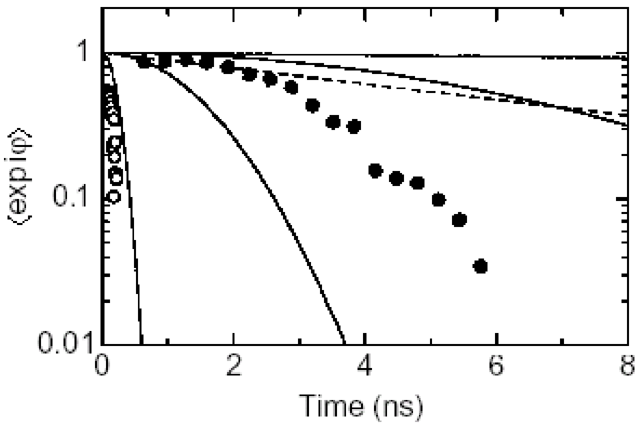

FIG. 3. Decay of the normalized amplitude of the echo signal (filled circles) and the FID signal (open circles) compared with estimated decoherence factors $\langle \exp i\varphi \rangle$ due to electromagnetic environment (dotted line), the read-out process (dashed), and $1/f$ charge noise with $\alpha = (1.3 \times 10^{-3}e)^2$ (dash-dotted). Two solid lines are estimations for the echo experiment in the presence of the same $1/f$ charge-noise spectrum (bottom) and that with $\alpha = (3.0 \times 10^{-4}e)^2$ (top).

Quantum oscillations in two coupled charge qubits

Yu. A. Pashkin, T. Yamamoto, O. Astafiev, Y. Nakamura, D. V. Averin & J. S. Tsai

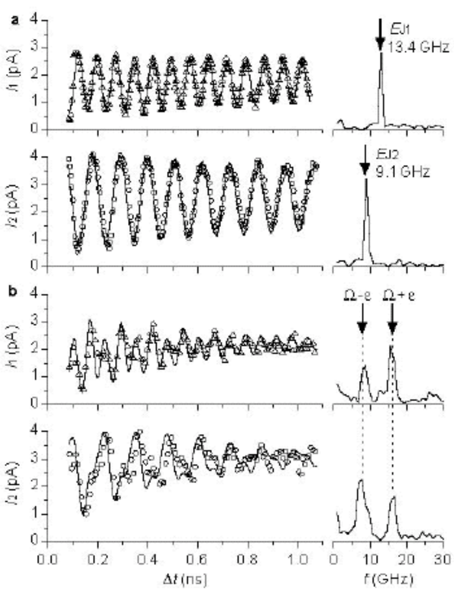

Figure 3. Quantum oscillations in qubits. **a**, Probe current oscillations in the first (top) and the second (bottom) qubit when the system is driven to the points R and L, respectively. Right panel shows corresponding spectra obtained by the Fourier transform. In both cases, the experimental data (open triangles and open dots) can be fitted to a cosine dependence (solid lines) with an exponential decay with 2.5 ns time constant. **b**, Probe current oscillations in the qubits at the co-resonance point X. Their spectra (right panel) contain two components. Arrows and dotted lines indicate the position of Ω + ε, Ω - ε obtained from (3) using E_{J1}=13.4 GHz, E_{J2}=9.1 GHz measured in the single qubit experiments (Fig. 3a) and E_m=15.7 GHz estimated independently from dc measurements. Solid lines are fits obtained from numerical simulation with the parameters E_{J1}=13.4 GHz, E_{J2}=9.1 GHz and E_m=14.5 GHz. Finite pulse rise/fall time and not pure |00> initial condition were taken into account. The introduced exponential decay time is 0.6 ns.

$\square_{\text{coupled}} \; \square \; \frac{1}{4}\square_{\text{uncoupled}}$

Quantum oscillations in two coupled charge qubits

Yu. A. Pashkin, T. Yamamoto, O. Astafiev, Y. Nakamura, D. V. Averin & J. S. Tsai

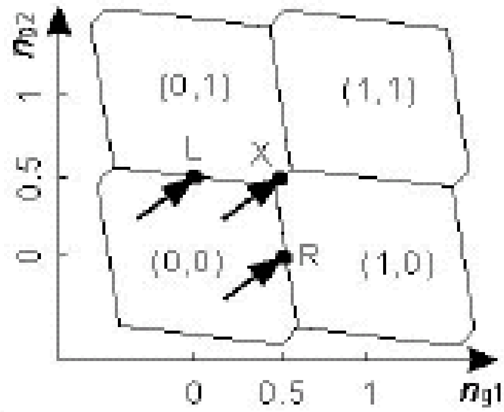

Schematics of the ground-state charging diagram of the coupled qubits as a function of the normalised gate charges n_{g1} and n_{g2}. The number of Cooper pairs n_1 and n_2 in the neighbouring cells differs by one. The electrostatic energies E_{n1n2} are degenerate at the boundaries. Points R and L correspond to energy degeneracy in the first and the second qubit, respectively. Point X is doubly degenerate: $E_{00} = E_{11}$ and $E_{10} = E_{01}$. Arrows show how pulses shift the system in the experiment.

Quantum oscillations in two coupled charge qubits

Yu. A. Pashkin, T. Yamamoto, O. Astafiev, Y. Nakamura, D. V. Averin & J. S. Tsai

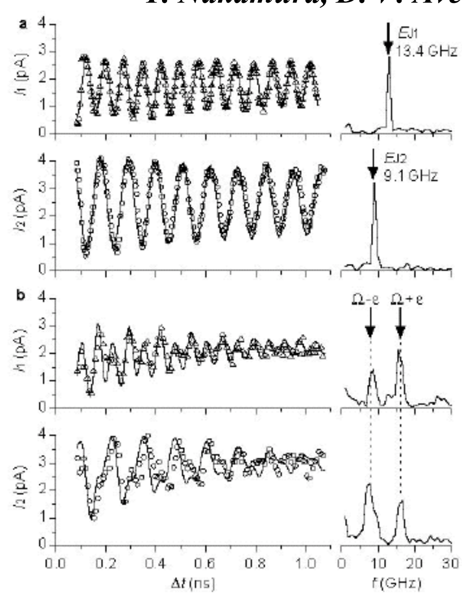

(0,0) [(1,0)

+

(0,0) [(0,1)

is not distinguished from

(0,0) [(1,1)

Decoherence of a spin 1/2

Consider a spinor
(total phase is irrelevant)

$$\psi = \begin{pmatrix} |\psi_\uparrow| e^{i\varphi} \\ |\psi_\downarrow| e^{-i\varphi} \end{pmatrix}$$

Average components of the spin can be expressed through the absolute values of the spinor's components and the phase

$$S_z = |\psi_\uparrow|^2 - |\psi_\downarrow| \qquad S_x = \sqrt{1 - S_z^2}\cos\varphi \qquad S_y = \sqrt{1 - S_z^2}\sin\varphi$$

A random time-dependent magnetic field $\vec{B}(t)$ changes the phase in an uncontrollable way ⟷ it rotates the spin.

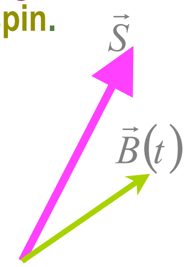

This can be called ***decoherence***

However

A classical magnet also gets rotated by external magnetic fields

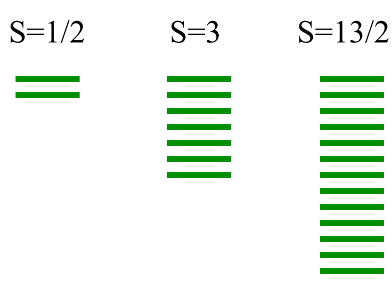

S>>1 – classical limit
Harmonic oscillator

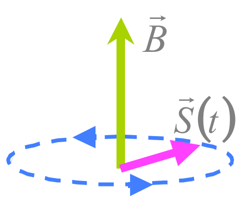

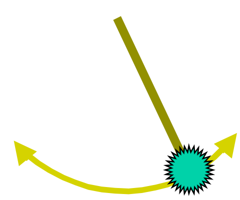

Just some oscillations is not exclusively a quantum effect!

For the quantum computation two-level systems (**S=1/2**) are necessary. Involvement of highly excited states is not permissible

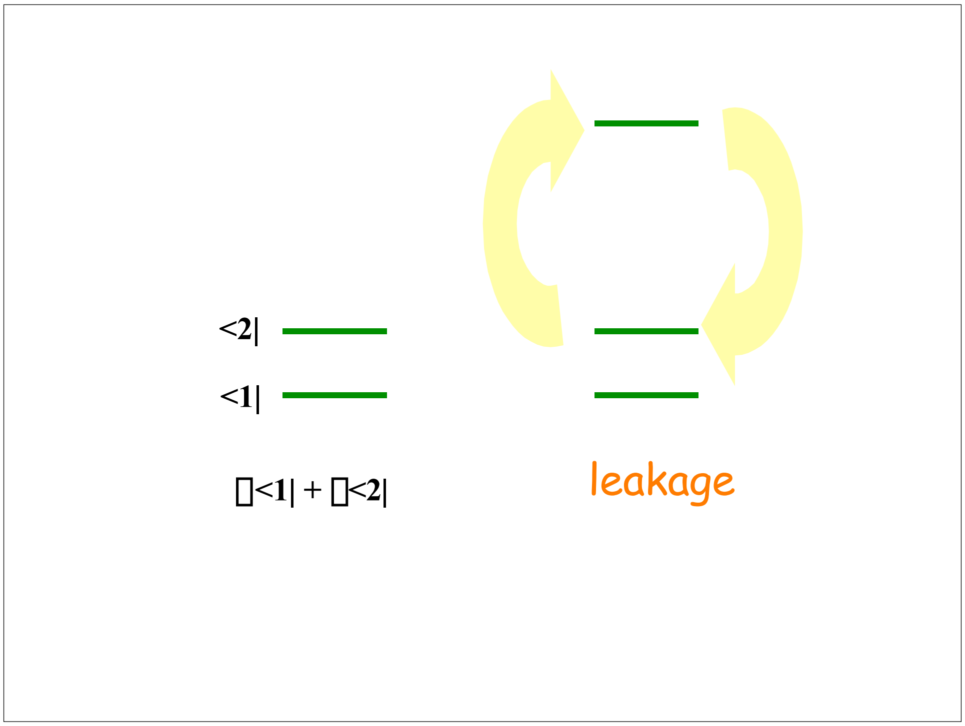
<2|
<1|
□<1| + □<2|
leakage

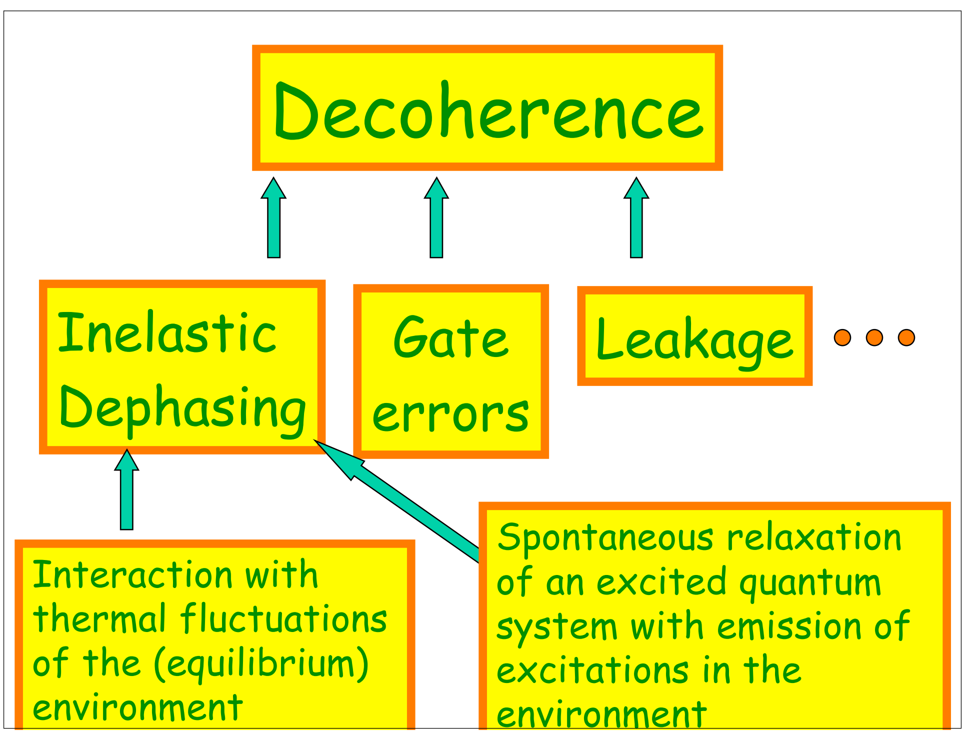
Decoherence
Inelastic Dephasing
Gate errors
Leakage
Interaction with thermal fluctuations of the (equilibrium) environment
Spontaneous relaxation of an excited quantum system with emission of excitations in the environment

Inelastic dephasing

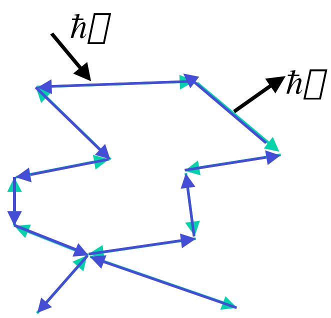

- other electrons
- phonons
- magnons
- two level systems
-
-

Can be modeled, e.g., by an interaction with an oscillator bath

Persistent current

$$J = \frac{\partial E}{\partial \Phi}$$

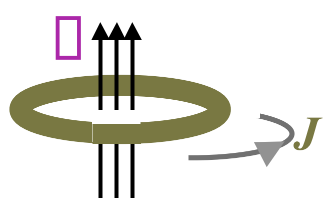

E **is the ground state energy**

Completely quantum phenomenon !?

Persistent current at zero temperature is a property of the ground state!

$$J = \frac{\partial E}{\partial \Phi}$$

E is the ground state energy

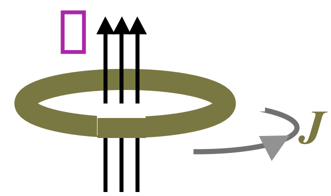

Interaction between electrons can change both E and J, but this does not mean that there is dephasing of the ground state wave function.

Measurements of the persistent current as well as of other **thermodynamic** properties **do not** allow to extract the dephasing rate.

VOLUME 18, NUMBER 24 PHYSICAL REVIEW LETTERS 12 JUNE 1967

INFRARED CATASTROPHE IN FERMI GASES WITH LOCAL SCATTERING POTENTIALS

P. W. Anderson
Bell Telephone Laboratories, Murray Hill, New Jersey
(Received 27 March 1967)

We prove that the ground state of a system of N fermions is to the ground state in the presence of a finite range scattering potential, as $N \to \infty$. This implies that the responce to application of such a potential involves only emission of excitations into the continuum, and that certain processes in Fermi gases may be blocked by orthogonality in a low-T, low-energy limit.

VOLUME 18, NUMBER 24 PHYSICAL REVIEW LETTERS 12 JUNE 1967

INFRARED CATASTROPHE IN FERMI GASES WITH LOCAL SCATTERING POTENTIALS

P. W. Anderson
Bell Telephone Laboratories, Murray Hill, New Jersey
(Received 27 March 1967)

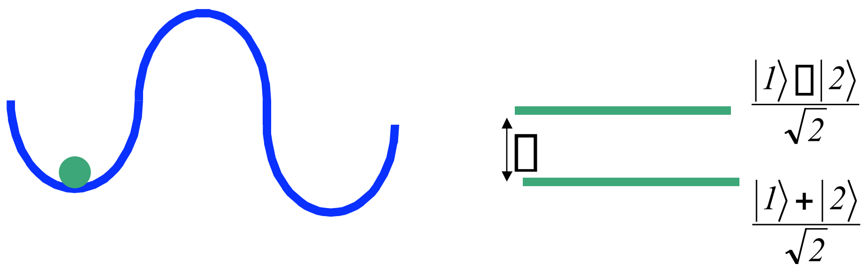

Interaction with the environment suppresses the tunneling, i.e., the splitting.

Is it a dephasing?

Typical problem/mistake:

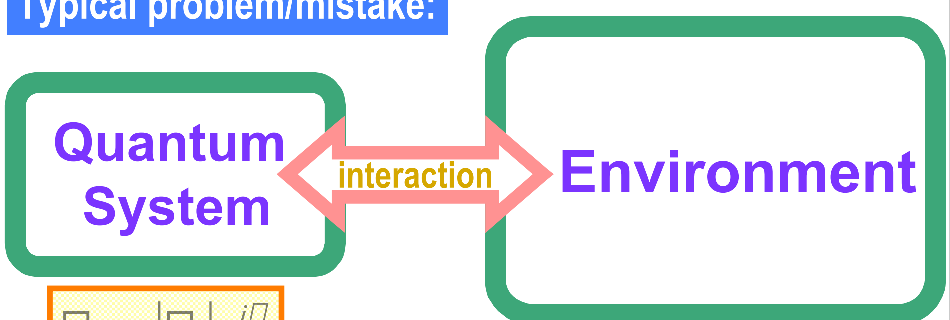

$$\Psi = |\Psi| e^{i\varphi}$$

Nobody yet invented device that can universally serve as a "phasometer".

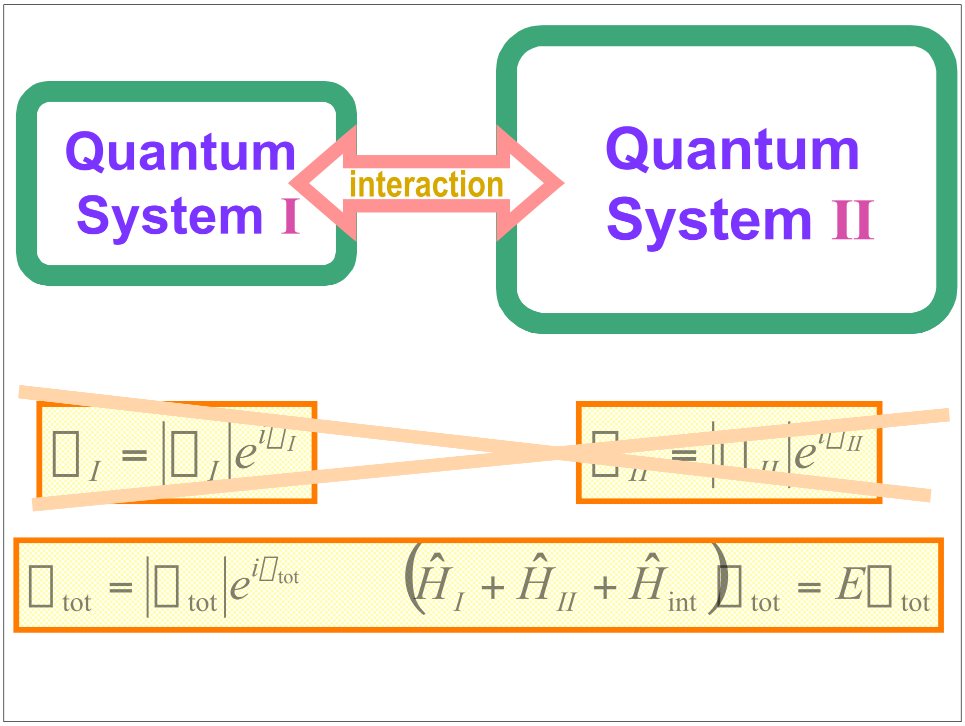
Quantum System I
interaction
Quantum System II

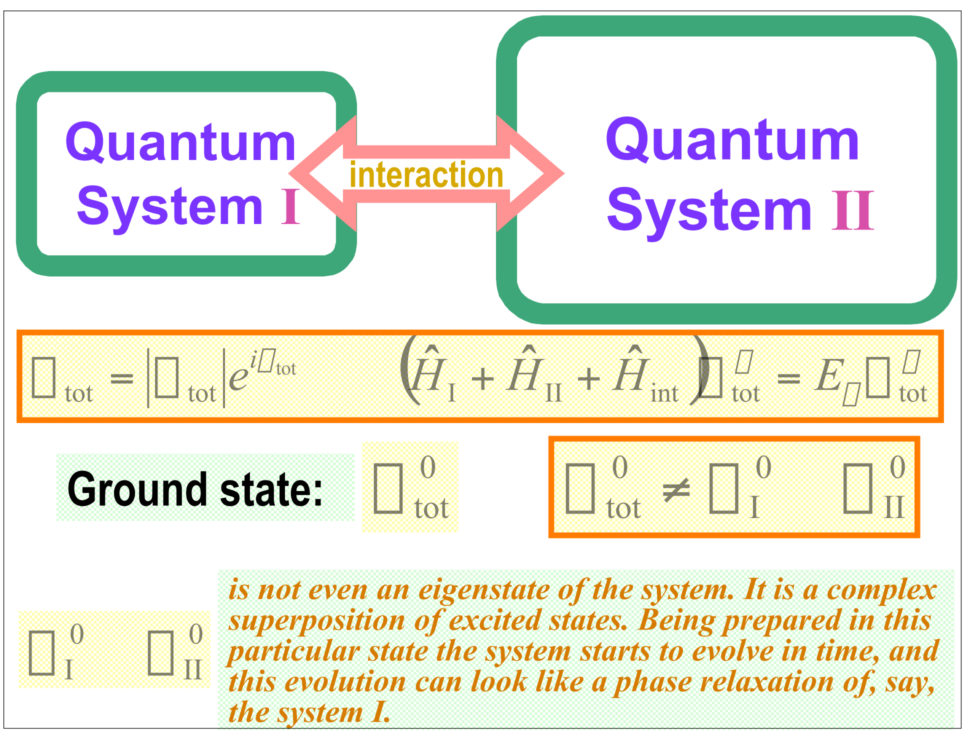
Quantum System I
interaction
Quantum System II
Ground state:
is not even an eigenstate of the system. It is a complex superposition of excited states. Being prepared in this particular state the system starts to evolve in time, and this evolution can look like a phase relaxation of, say, the system I.

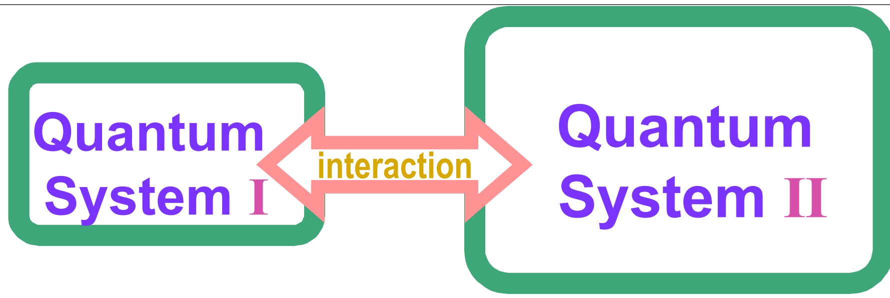

Ground state: Ψ^0_{tot} $\quad \Psi^0_{tot} \neq \Psi^0_{I}\ \Psi^0_{II}$

$\Psi^0_{I}\ \Psi^0_{II}$ *is not even an eigenstate of the system. It is a complex superposition of excited states. Being prepared in this particular state the system starts to evolve in time, and this evolution can look like a phase relaxation of, say, the system I.*

Q: Does it mean that there is zero temperature dephasing ?

A: No

Inelastic dephasing

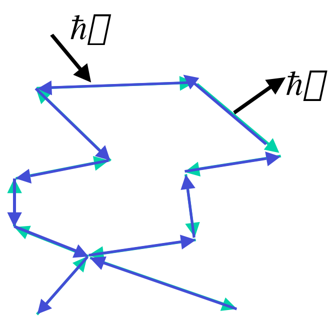

- other electrons
- phonons
- magnons
- two level systems
-
-

Can be modeled, e.g., by an interaction with an oscillator bath

e-e interaction – Electric noise

Fluctuation- dissipation theorem:

Electric noise - randomly time and space - dependent electric field $E^{\alpha}(\vec{r},t) \to E^{\alpha}(\vec{k},\omega)$ **.**
Correlation function of this field is completely determined by the conductivity $\sigma(\vec{k},\omega)$ **:**

$$\left\langle E^{\alpha}E^{\beta}\right\rangle_{\omega,\vec{k}} = \frac{\omega}{\sigma_{\alpha\beta}(\omega,\vec{k})}\coth\left(\frac{\omega}{2T}\right)\frac{k_{\alpha}k_{\beta}}{k^2} \approx \frac{T}{\sigma_{\alpha\beta}(\omega,\vec{k})}$$

Noise intensity increases with the temperature, T, and with resistance

$$\left\langle E^{\alpha}E^{\beta}\right\rangle_{\omega,\vec{k}} = \frac{\omega}{\sigma_{\alpha\beta}(\omega,\vec{k})}\coth\left(\frac{\omega}{2T}\right)\frac{k_{\alpha}k_{\beta}}{k^2} \approx \frac{T}{\sigma_{\alpha\beta}(\omega,\vec{k})}$$

Dephasing rate due to e-e interaction for 1d and 2d cases

$g(L) \equiv \frac{h}{e^2 R(L)}$ *- Thouless conductance – def.*

$R(L)$ *- resistance of the sample with* { *length (1d)* / *area (2d)* } L

$$\frac{1}{\tau_{\varphi}} \approx \frac{T}{g(L_{\varphi})}$$

$L_{\varphi} \equiv \sqrt{D\tau_{\varphi}}$ *- dephasing length*

D *- diffusion constant of the electrons*

$$\frac{1}{\tau_\varphi} \approx \frac{T}{g(L_\varphi)}$$

Fermi liquid is valid (one particle excitations are well defined), provided that

$$T\tau_\varphi(T) > \hbar$$

1. *In a purely* ***1d*** *chain,* $g \sim 1$ *,and, therefore, Fermi liquid theory is never valid.*

2. *In a multichannel wire* $g(L_\varphi) > 1$ *,provided that* L_φ *is smaller than the localization length, and Fermi liquid approach is justified*

$$\frac{1}{\tau_\varphi} \approx \frac{T}{g(L_\varphi)}$$

$$g(L) \propto L^{d-2}$$

$$L_\varphi \propto \sqrt{\tau_\varphi}$$

where is the number of dimensions:
$d=1$ *for wires;* $d=2$ *for films, …*

$$L_\varphi \propto T^{-1/(4-d)}$$

$$\tau_\varphi \propto T^{-2/(4-d)} \quad \begin{cases} T^{-1} & d=2 \\ T^{-2/3} & d=1 \end{cases}$$